International Journal of Mechanical Design and Materials Science

Volume 1, Issue 3 2025

In ductile cellular solids, size impacts. Part II: Results of the experiment

Xue-Feng ,Liu. Department of Design ,china

Research Article

Date of Submission: 10-04-2025 Date of Acceptance: 19-05-2025 Date of Publication: 1-06-2025

Abstract

The usage of metallic foams in a range of applications, such as energy absorption devices and lightweight structural sandwich panels, is gaining popularity. The foams' mechanical responsiveness is crucial in these kinds of applications. In this work, we have examined how certain mechanical characteristics of aluminum foams are affected by specimen size (in relation to cell size). A physical foundation for comprehending size effects in metallic foams is provided by models, which are detailed in the companion article. Size effects in metallic foams are well described by the models.

Keywords: Size effects, mechanical properties, and cellular solids

Introduction

For more than 40 years, metallic foams have been around [1]. Interest in their usage in a range of applications, including as energy absorption devices and lightweight structural sandwich panels, has grown due to the discovery of many less expensive production methods. These more recent metallic foams' mechanical response, which is crucial in these kinds of applications, is presently being assessed [2–10]. The impact of specimen size in relation to cell size on measured parameters is a significant concern in mechanical testing of foams. Since certain components may only be a few cell diameters (usually d~2–6 mm), the size impact is equally significant in design. In the preceding companion study, we examined how the uniaxial, shear, and indentation responses of regular, hexagonal honeycombs were affected by the ratio of specimen size to cell size, or L/d. Up to a plateau level that corresponds to the bulk characteristics, it was discovered that the Young's modulus and uniaxial strength increased with rising L/d values. Both the rising area fraction of stress-free cell walls and the decreased constraint of cell walls at the free surface contributed to the decreased stiffness and strength at lower L/d values. The function of a stiff border on two parallel sides was investigated in the shear modulus and strength model. This time, the greater restriction of the cell walls at the boundary causes the shear moduli and strength to drop as L/d increases. A honeycomb's indentation load is the total of the force needed to crush the honeycomb below the indenter and the force needed to yield and then break the cell walls around the indenter's perimeter so that it may pass through the honeycomb. The inverse of the indenter width affects the indentation strength. By simulating the mechanics behind the size effects, the findings for honeycombs were expanded to foams. In this study, we provide observations of how specimen size (in relation to cell size) affects the mechanical characteristics of aluminum foams, including Young's modulus, uniaxial compression strength, shear strength, and indentation strength. The models developed in the companion study [14], which provide a physical foundation for comprehending size effects in metallic foams, are compared with the data.

Experimental procedure

Materials

The mechanical testing was conducted using a nominally 7% dense, 20 pore per inch, open-cell aluminum (6101-T6) foam (brand name Duocel; ERG, Oakland, CA) and a nominally 8% dense, closed-cell aluminum foam (trade name Alporas; Shinko Wire, Amagasaki, Japan). Numerous research have examined their mechanical and microstructural characteristics [3,6–8,11]. The cells of the open-cell foam are stretched in a single direction. Calipers were used to measure the cell size on cylindrical specimens that were 6 mm in diameter and 12 mm in height. The tiny number of cells inside the specimens made it possible to estimate the cell size. It was discovered that the cell size was around 3.0 mm perpendicular to the axis of cell elongation and 4.5 mm parallel to it. According to earlier measurements made using the mean intercept length approach, the closed cell foam's cell size is 4.5 mm in each of the three directions [6]. The mechanical characteristics of both foams are transversely isotropic. The specimens' orientation did not change throughout a particular series of testing. Every time the open-cell foam was tested, the loading direction was parallel to the cell elongation axis. Square prisms of the closed-cell foam and cylinders of the open-cell material were used to examine the impact of specimen size on the compressive modulus and strength. On the closed-cell foam, the impact of specimen size on shear strength and indentation strength was investigated. The density of the foam was determined for every sample in every test using the sample's measured mass and size. The open-cell foam specimens had a density of 197 kg/m³ (with a standard variation of 11.6 kg/m³), while the closed-cell foam specimens had a density of 223 kg/m³ (with a standard deviation of 8.3 kg/m³).

Uniaxial compression tests

Square prisms of the closed-cell foam with height (H) equal to twice the cross sectional size (L) were used to assess the compressive Young's modulus and plastic collapse strength. For every test, the specimen geometry remained the same, but the absolute dimensions were changed such that L=8, 12, 17, 24, 30, 36, and 50 mm. Using a band saw with a guide to guarantee precise and straight cuts, specimens were cut to the proper proportions. Each size was examined on five to nine specimens. An Instron testing apparatus (Model 4201, Instron, Canton, MA) with a 5 kN load cell was used for the compression tests. The displacement and load data from the Instron machine were obtained for further processing using the software program Labview (National Instruments, Austin, TX). Steel loading platens were used to crush the specimens. The loading was carried out under displacement control at a loading rate that resulted in an applied strain rate of 1×10^{3}/s in every test. Every specimen was loaded to a strain of around 20%, which was much higher than the initial yield strain of about 2-3% but still before the densification strain, which is typically between 60 and 70%. The specimen was emptied for each test shortly before plastic collapse began, then reloaded, and the test proceeded until the last strain.

The purpose of this was to evaluate the elastic unloading modulus. The applied stress was calculated by dividing the applied load by the original specimen area, and the strain was calculated by dividing the specimen displacement by the original specimen height. By deducting the displacement associated with the testing machine compliance from the measured cross-head displacement, the specimen displacement was calculated. To evaluate the test machine compliance, a different test was conducted without a specimen. It was discovered that the displacement related to the test machine compliance was just 5% of the overall cross-head displacement at the low load levels involved in these foam tests.

In the closed-cell Alporas foam, localized bands of collapsed cells are shown to start forming at stresses of around half the plateau stress, resulting in inhomogeneous deformation and strain. The average strain over the specimen is what we assess in our testing. The unloading modulus, which is the measurement presented here, may be used to circumvent the effects of localized plasticity on modulus measurements.
Additionally, cylinders of the open-cell foam with a height to diameter ratio of two were subjected to compression testing. The parameters of the cylinder diameter were 6.4, 12.7, 19.0, 25.4, and 50.8 mm. An Instron testing apparatus was used to test three to five specimens of each size. Since the smaller specimens could not be fitted with an extensometer, displacement was quantified using the crosshead displacement. The bigger specimens were fitted with an extensometer for comparison; the moduli recorded with the extensometer were around 10% more than those obtained with the crosshead. In every instance, the Young's moduli were computed using the crosshead displacement. The slope of the unloading stress-strain curve at a stress of around 0.75 times the compressive plateau stress was used to calculate the Young's modulus.

Shear tests

The shear strength of the closed cell aluminum foam was measured according to ASTM C-273 (Standard Test Method for Shear Properties of Sandwich Core Materials). Five different thick-nesses of specimen were tested (6, 12, 18, 24, and 30 mm); the ratio of length to thickness was constant at $l/t=12$. All of the specimens were of constant width of 50 mm. Five specimens of the 6 mm thick specimens and six specimens of the thicker specimens were tested. The specimens were
cut using a band saw and bonded to 12 mm thick milled aluminum plates using a structural adhesive film (FM300, Cytec, Havre de Grace, MD). The adhesive between the specimens and the
plates was cured in an autoclave at a pressure of 0.14 MPa and a temperature of 177°C for 1 h. The shear tests were carried out in an Instron testing machine (Model 1321 , Instron, Canton, MA) with a 50 kN load cell in displacement control such that the imposed strain rate was about 3×10^{-a}/s.

Displacement was measured using LVDTs mounted on the plates. Displacement and load signals
were acquired using LabView. The shear strength was taken as the peak stress. All specimens were loaded to failure which occurred at a strain of about 2–4%.

Indentation tests

Axisymmetric indentation tests were carried out on the closed-cell aluminum foam using cylindrical indenters of 6, 12, 24, and 30 mm diameter and between 12 and 20 mm in height. The cylinders were indented up to about 5 mm into a block of foam which was 1.5–3 times the indenter diameter in depth. Each indentation was made at least one indenter diameter away from any other indentations. Preliminary tests showed that this distance was sufficient to avoid edge effects or interference effects between indentations. The indentation tests were performed in an Instron testing machine (Model 1361, Instron, Canton, MA) with a 10 kN load cell at a loading rate of
0.05 mm/s. Displacement was measured from the crosshead displacement and both load and displacement data were acquired using Labview software. At least five indentations were performed for each size of indenter. The indentation stress was calculated from the first peak stress in the load–deflection curve.

Results

Typical compressive stress–strain curves for the open- and closed-cell foams, illustrating the unloading response and the initial peak stress, or the plastic collapse stress, are shown in Fig. 1. For the closed-cell foam (Alporas), the slope of the loading curve is less steep than that of the unloading
curve, indicating that plastic deformations occur even at stresses well below the plastic collapse strength; this observation is consistent with those of other studies [2,3,6]. Young's modulus is taken as the slope of the unloading curve. The shape of the stress–strain curve is typical of this material, showing an increase up to a peak load, then a drop to a region of more or less constant stress with slight oscillations about the constant stress. For the open-cell foam (Duocel), the stress–strain curve is linear up to the elastic limit. The slope of the initial linear portion of the curve is equal to that of the unloading curve. Beyond the elastic limit the curve is non-linear and reaches a peak stress at a strain of about 1%, after which the stress remains roughly constant. For each material, the shape of the curve was similar for the entire range of specimen sizes, although the actual values of stiffness and strength varied for the different specimen sizes.

The average density, Young's modulus and compressive strength for each size of specimen tested are listed in Table 1. The Young's modulus and peak stress, normalized by those of the bulk
material, are plotted against the specimen size, L, relative to the cell size, *d*, in Figs. 2 and 3.

The modulus increases with increasing normalized specimen size up to a plateau level at L/*d*≈6 for both foams. The modulus of the bulk material was taken as the average value for L/*d*>6 (E_{a511}=943 MPa for Alporas and E_{a511}=368 MPa for Duocel). For L/*d*<6, the Young's
modulus of the open-cell foam drops more rapidly with decreasing L/*d* than that for the closed-cell

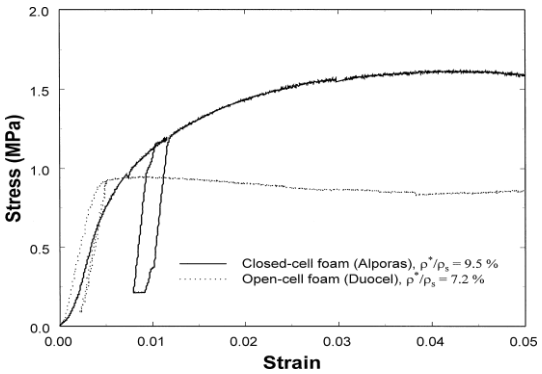


Fig. 1. Typical compressive stress–strain curves for closed cell (Alporas) and open cell (Duocel) aluminum foam.

Table 1
Uniaxial compression data for specimens of varying size

L (mm)	Density (g/mm³)	$E_{5_{n^{1oaa}}}$ (MPa)	σ_{pH_l} (MPa)
Alporas foam results			
Square prisms L×L×2L			
50	0.2175 (0.0018)	943 (27)	1.51 (0.02)
36	0.2169 (0.0018)	913 (24)	1.44 (0.05)
30	0.2276 (0.0016)	910 (39)	1.48 (0.04)
24	0.2290 (0.0016)	792 (39)	1.47 (0.05)
17	0.2282 (0.0041)	612 (69)	1.18 (0.11)
12	0.2169 (0.0054)	652 (76)	1.07 (0.06)
8	0.2277 (0.0166)	384 (58)	0.95 (0.19)

Duocel foam results Specimens: Cylinders, H=2D

D (mm)	Density (g/mm³)	$E_{5_{n^{1oaa}}}$ (MPa)	$\sigma_{p}H_{l}$ (MPa)
50.8	0.1863 (0.0027)	357 (6)	1.35 (0.07)
25.4	0.1877 (0.0046)	379 (39)	1.37 (0.25)
19.05	0.2003 (0.0086)	369 (90)	1.19 (0.42)
12.7	0.2014 (0.0095)	287 (61)	1.00 (0.06)
6.35	0.2052 (0.0159)	118 (52)	0.56 (0.27)

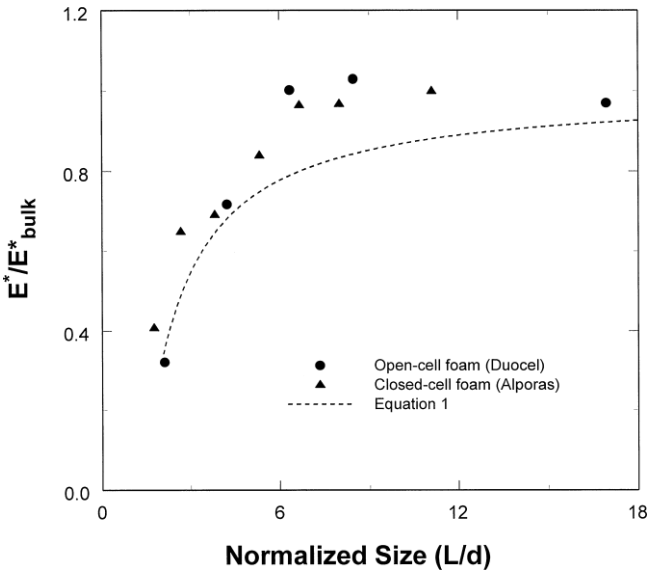


Fig. 2. Unloading Young's modulus, normalized by the bulk value, plotted against specimen edge length, L, normalized by the cell size, *d*, for the open- and closed-cell aluminum foams.

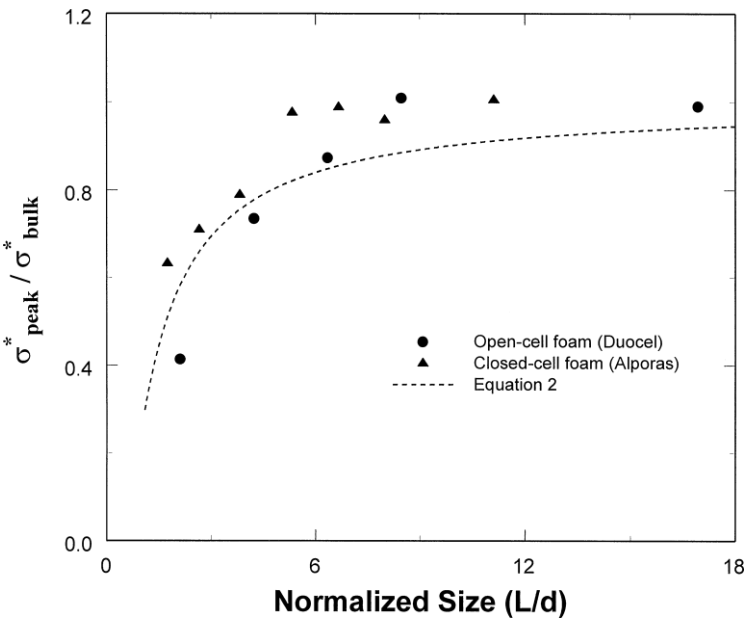


Fig. 3. Plastic collapse strength, normalized by the bulk value, plotted against specimen diameter, L, normalized by the cell size, *d*, for the open- and closed-cell aluminum foams.

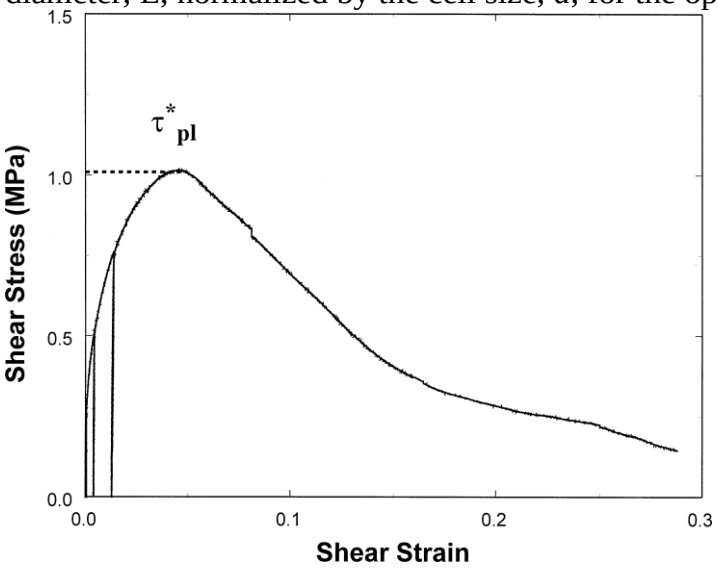


Fig. 4. Typical shear stress–shear strain curve for the closed-cell aluminum foam (Alporas) (*t*=30 mm). foam. The normalized peak stress follows a similar pattern, increasing with L/*d* up to a plateau level at L/*d*=8 for the open-cell foam and at L/*d*=5 for the closed-cell foam. At lower values of L/*d*, the peak stress of the open-cell foam falls more rapidly with decreasing L/*d* than that for the closed cell foam. The peak stress of the bulk material was taken as the average value for
L/*d*>8 or 5 for the open- and closed-cell foams, respectively ($\sigma_{pl}^{*} = 1.35$ MPa for Duocel and $\sigma_{pl}^{*} = 1.51$ MPa for Alporas). The bulk values for both the Young's modulus and the peak stress are comparable to those measured by Simone and Gibson [6] on 50 mm×50 mm×100 mm
prisms.

A typical shear stress–strain curve for the closed-cell foam (Alporas) is shown in Fig. 4. The shear strength, normalized by the bulk value, is plotted against the ratio of specimen thickness, *t*, to cell size, *d*, in Fig. 5. The average density of the 12, 18, 24 and 30 mm specimens was 212 kg/m³ with a standard deviation of about 8 kg/m³. The densities of the five 6 mm thick specimens were significantly lower: 180, 182, 183, 189 and 210 kg/m³. The average shear strength of the three lower density 6 mm thick specimens was 1.11 MPa, compared with 1.36 MPa for the 189 kg/m³ and
1.64 MPa for the 210 kg/m³ density specimens. Density variations between specimens of different thicknesses were minimized by reporting, for each thickness over 6 mm, the average shear strength of the three specimens with densities closest to 200 kg/m³.

The individual data points for the 189 and 210 kg/m³ densities of the 6 mm specimens are plotted on Fig. 5: their average shear strength is
1.50 MPa. The shear strength of the thicker specimens is roughly constant at a value of 1.02 MPa. The shear strength becomes independent of the specimen thickness at t/d=2.67.
A typical stress–displacement curve for an indentation test is shown in Fig. 6. The indentation stress, reached at a displacement of about 1mm, is roughly constant. The indentation stress,

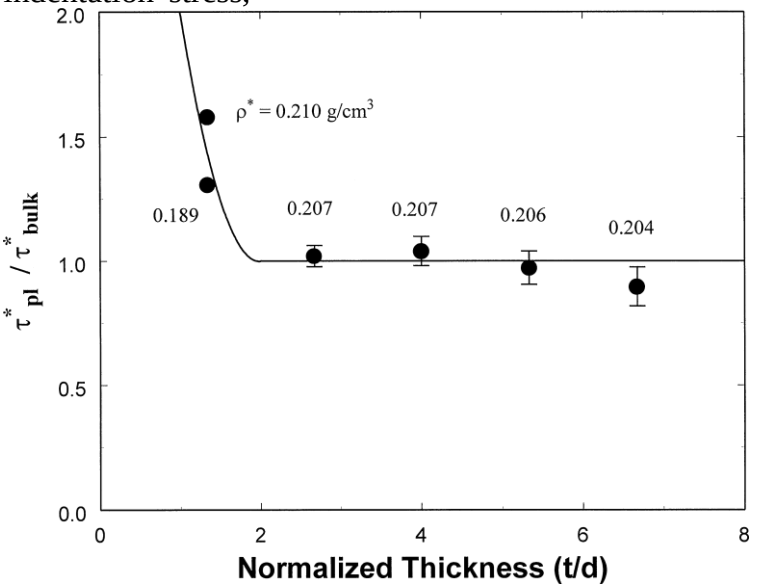


Fig. 5. Shear strength, normalized by the bulk value, plotted against the ratio of specimen thickness, t, to the cell size, d, for the closed-cell foam (Alporas).

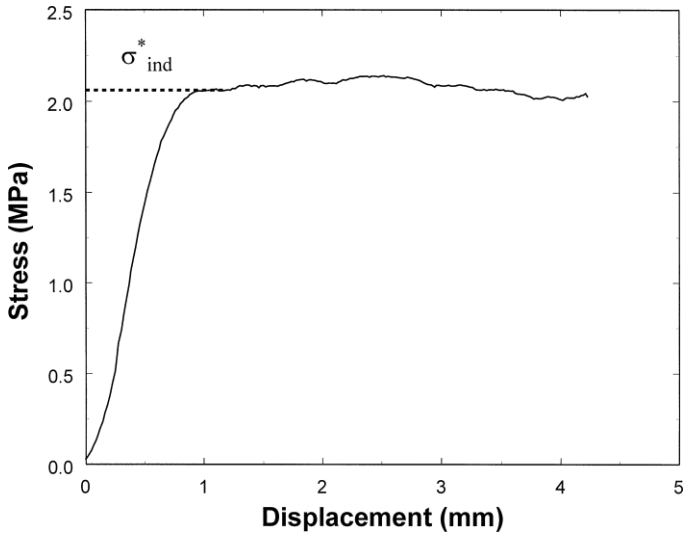


Fig. 6. Indentation stress–displacement curve for the closed-cell foam (Alporas) for an indenter diameter of 30 mm. normalized by the plastic collapse strength, is plotted against the ratio of indenter diameter, *D*, to cell size, *d*, in Fig. 7: it increases as the inverse of the indenter diameter. The value of the indentation stress for large indenter diameters approaches a value slightly higher than the uniaxial compressive strength of the material (1.42 MPa).

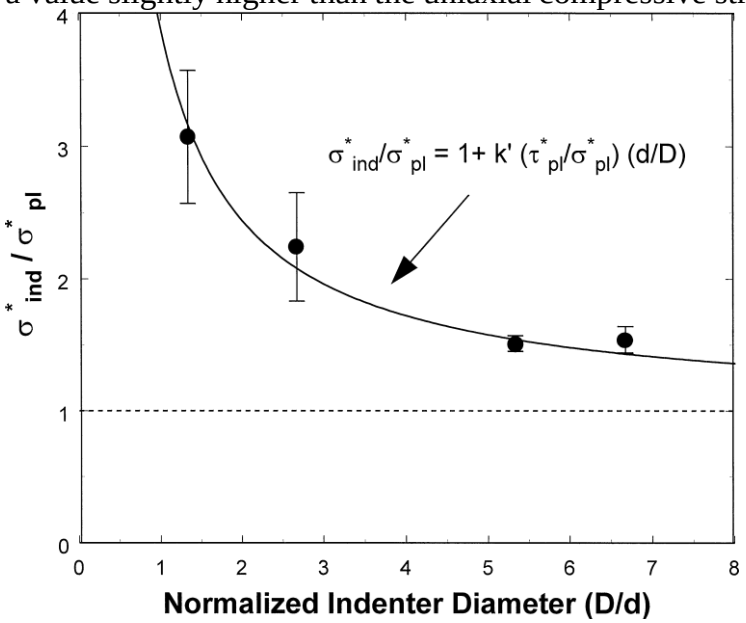


Fig. 7. Indentation peak stress, normalized by the plastic collapse strength, plotted against the ratio of indenter diameter, *D*, to cell size, *d*, for the closed-cell aluminum foam (Alporas).

The solid line represents Eq. (3).

Discussion

Uniaxial compression

The effect of the ratio of specimen size to cell size on the Young's modulus of a honeycomb was analyzed in the previous companion paper by considering two contributions: the decreased constraint at the free surface of the foam, giving a less stiff boundary layer, and the area fraction of cut cell walls at the boundary which remain stress-free. For a foam, both effects give (Eq. (35) of the previous, companion paper) [14]

$$\frac{E}{E_{a511}} = \left(1 - 2n\frac{d}{L} - 2p\frac{d}{L}\right)^2 + 4nm\left(\frac{d}{L}\right)\left[1 - 2n\frac{d}{L} - 2p\frac{d}{L}\right] + 4n^2m^2\left(\frac{d}{L}\right)^2 \quad (1)$$

where *m* is the reduced stiffness factor for the boundary layer of thickness *nd* and the stress free layer of zero stiffness is of thickness *pd*. Eq. (1) is plotted on Fig. 2 with *m*=0.85, *n*=0.5 and *p*=0.25; it follows the general trend of the data but reaches the plateau value for the modulus at higher values of L/*d*.

The normalized moduli for the open-cell foam decrease more rapidly with decreasing L/*d* than those for the closed-cell foam. Two factors contribute to this. The cell faces in the closed-cell foam may increase the stiffness of its boundary layer compared with that for the open-cell foam. And the cut cell edges of the open-cell foam are stress-free, like those of the honeycomb, while the cut cell

edges and faces at the boundary of the closed cell foam are not completely stress-free, due to the presence of the faces.

The size effect for the uniaxial compressive strength of a honeycomb arises from the stress-free walls at the boundary of the honeycomb. Analysis of the same phenomenon in foams gives [14]

$$\frac{\sigma_{p1}}{\sigma_{pH_1}} = \frac{\overline{(L/d - 1/2)2}}{(L/d)2}. \quad (2)$$

Eq. (2) is plotted along with the data shown in Fig. 3; it describes the data well. We note that the normalized strength decreases more rapidly with decreasing L/*d* for the open-cell than the closed-cell foam, again, due to the effect of the cell faces.

Both our data and models suggest that the bulk values of both Young's modulus and strength are reached at values of L/*d* of about 5–8, lower than the value of 15 suggested by Brezny and Green [12]. The discrepancy may be due to a difference in test methods. They used three point

bend specimens which subject the more compliant top and bottom surfaces of the beam to the highest normal stresses, magnifying the size effect in smaller beams and increasing the critical value of L/*d*. Their tests were performed on a brittle reticulated vitreous carbon foam which exhibits a Weibull size effect, confounding the specimen size/cell size effect.

The trends we observe in stiffness and strength are similar to those of Bastawros et al. [13]. In that study, uniaxial compression tests were performed on prismatic aluminum foam specimens of constant length and width and varying depth. They found that stiffness and strength became essentially constant when the depth was greater than about 4 times the cell size.

Shear strength

The normalized shear strength of the closed-cell foam decays rapidly to a plateau value at a ratio of the specimen thickness to cell size, *t*/*d*, of 2.

Since there are no stress or strain gradients in the out-of-plane direction in the shear test, the two-dimensional honeycomb analysis of size effects on shear strength can be applied directly to foams. Assuming that, on average, the cell edges and faces are cut at the midpoint along their length, the honeycomb analysis indicates that $\tau_{pl}/\tau_{as11} = 2$ for $t/d=1$, and that τ_{pl}/τ_{as11} decays to a value of unity for $t/d \approx 2$ [14], in close agreement with our experimental results (Fig. 5).

Indentation

The indentation stress varies with the inverse of the indenter diameter, D. In an indentation test, the foam immediately below the indenter crushes and the foam at the perimeter of the indentation yields in shear and then ruptures (Fig. 8). The total force on the indenter is the sum of the crushing force (equal to the plastic collapse strength of the foam times the cross sectional area) and the shearing force (equal to the shear strength of the foam times the perimeter)

$$P_{in} = P_{31531} + P_{31aa1} = \sigma H \frac{nD2}{P1\ 4\ P1} + k\tau H nDd$$

or

$$\sigma_i H_{na} = 1 + k' \left(\tau_P H_1 \right) d \quad (3)$$

$$\overline{\sigma H_{p1}} \quad \overline{\sigma_p H_1}\ \overline{D}$$

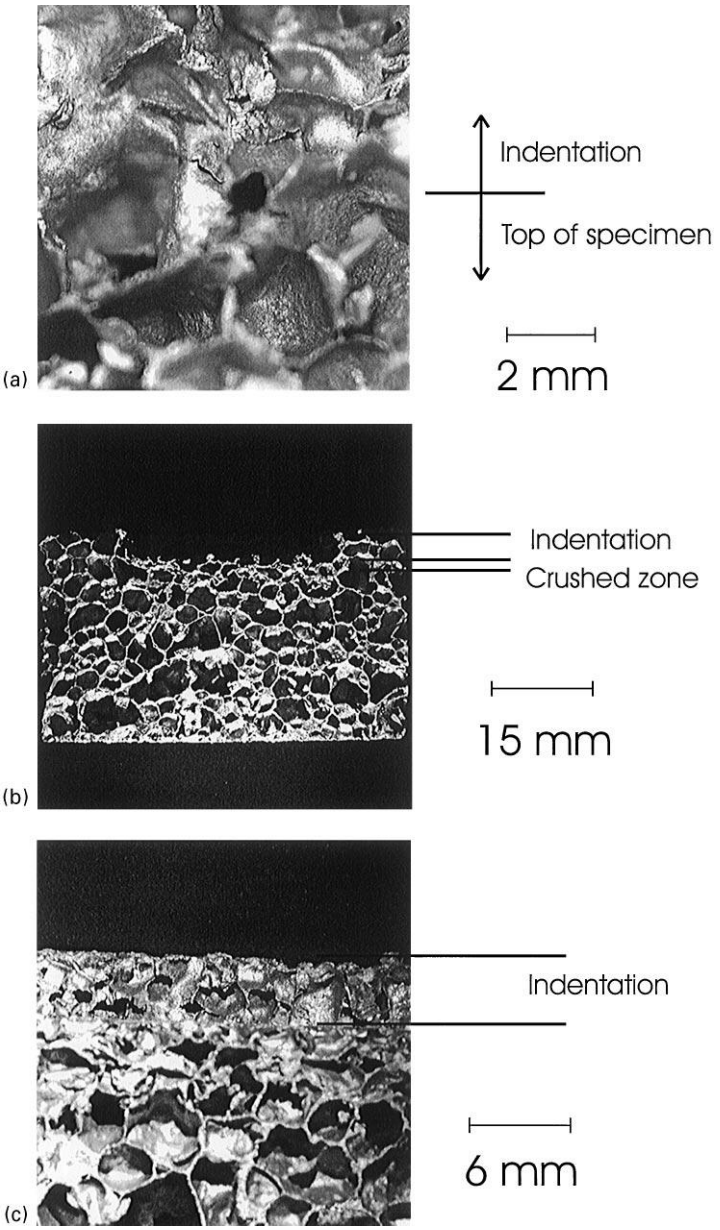


Fig. 8. Optical photographs of indentation specimens. (a) Specimen loaded to the initial peak stress and then unloaded. View from above the indentation showing torn cell walls at perimeter of indentation. (b, c) Longitudinal section of a specimen loaded beyond the initial peak stress and then unloaded, showing the indentation, the crushed zone beneath the indentation and torn cell walls on the back wall of the perimeter of the indentation.

Eq. (3) is compared with the indentation data in Fig. 7 using our measured values for
σ_{pl} = 1.42 MPa and τ_{pl} =1.03 MPa. We find a value of *k*'=3.98 from the fit of Eq. (3) to the data, giving *k*=1. This suggests that yielding at the boundary of the indenter extends to a depth of about
1 cell into the foam. The indentation data are well described by Eq. (3).

Conclusions

As the ratio of specimen size to cell size rose, the Young's modulus and plastic collapse strength of both the open-cell Duocel foams and the closed-cell Alporas climbed to a plateau level. The Young's modulus for both foams attained a plateau value at L/d=6, whereas the compressive strength of the open-cell and closed-cell foams reached a plateau value at L/d=8 and 5, respectively. Because of the influence of the cell faces, the modulus and strength of the open-cell foam fell more quickly with decreasing L/d than those of the closed-cell foam. The results for uniaxial loads are well described by extending the analytical models for size effects in honeycombs to foams.

For specimens that are at least twice as thick as the cell size, the size influence on shear strength disappears. The results for the closed-cell aluminum foam are well described by the two-dimensional honeycomb model for the influence of t/d on the shear strength, which is also applicable to foams.

As the indenter's size rises in relation to the cell size, the indentation strength declines and approaches a limiting value that is marginally more than the foam's uniaxial plastic collapse strength. The decline fluctuates according to the indenter diameter's inverse. This may be explained by the fact that during an indentation test, the cell walls at the indentation's perimeter yield and eventually burst, while the foam just under the indenter smashes. The data is well described by a basic model.

References

[1] Elliot JC. Metal foam production method. 1956 U.S. Patent No. 2,751,289.
[2] Gradinger R, Degischer HP, Simancik F. Mechanical characteristics of foamed metals are determined. Vienna University of Technology, International Conference on Welding Technology, Materials and Materials Testing, Fracture Mechanics, and Quality Management, 1997.
[3] Sugimura Y, Meyer J, He MY, Bart-Smith H, Grenestedt J, Evans AG. about closed cell foams' mechanical performance. Acta Materiala 45:5245–59, 1997.
[4] Bart-Smith H, Bastawros A-F, Mumm DR, Evans AG, Sypeck DJ, Wadley HNG. X-ray tomography and surface strain mapping were used to study compressive deformation and yielding processes in cellular Al alloys. Acta Materiala 46:3583–92, 1998.
[5] Ashby MF, Hutchinson JW, Evans AG. Cellular metal systems' multifunctionality. Materials Science Progress 43:171–221, 1998. Aluminum foams made by liquid state methods, Simone

AE, Gibson LJ. Acta Materiala 46:3109–23 (1998).
[6] von Hagen H, Bleck W. Shear, tensile, and compressive tests of melt-foamed aluminum. Symposium R: Cellular and Porous Materials for Structural Uses, Materials Research Society Spring Meeting, San Francisco, 1998.
[7] Andrews EW, Sanders W, Gibson LJ. Aluminum foams' compressive and tensile behavior. Materials Science and Engineering A 270:113–24, 1999.
[8] Deshpande, Fleck NA. Metallic foam isotropic constitutive models. Journal of Solid Mechanics and Physics 48:1253–83, 2000.
[9] Ashby MF, Fleck NA, and Harte A-M. Fatigue failure of aluminum alloy foam in both closed and open cells. [10] Gioux G, McCormack TM, Gibson LJ. Failure of aluminum foams under multiaxial stresses. Acta Materiala 1999;47:2511–24. Mechanical Sciences International Journal 42:1097–117, 2000.
[11] Green DJ, Brezny R. description of cellular materials' edge effects. Journal of Materials Science 25:4571–8, 1990.
[12] Evans AG, Bart-Smith H, and Bastawros A-F. Deformation processes in a closed-cell Al alloy foam are analyzed experimentally. Journal of Solid Mechanics and Physics 48:301–22, 2000.
[13] Onck PR, Andrews EW, Gibson LJ. Part I: Modeling of size effects in ductile cellular solids. Mechanical Sciences International Journal 43:681–99, 2001.